

# Heat conduction across double brick walls via BEM

Fernando Branco, António Tadeu\*, Nuno Simões

*Department of Civil Engineering, Faculty of Sciences and Technology, University of Coimbra, Pólo II,  
Pinhal de Marrocos, 3030-290 Coimbra, Portugal*

Received 15 May 2001; received in revised form 12 July 2003; accepted 6 August 2003

## Abstract

The Boundary Element Method (BEM) is used to compare the steady-state heat and moisture diffusion behaviour across double brick walls provided by two different models: in the first one, the brick wall is assumed to be composed of a set of homogeneous layers bonded together, which is the model frequently used to predict internal condensation; in the second model, the geometrical modelling and hygrothermal properties of the individual bricks are taken into account.

The BEM is implemented allowing the use of multi boundaries, which permits the full discretization of the brick cavities.

Three different construction solutions are analysed. In the first, the double-brick wall is assumed not to be thermally insulated; in the second, the space between the two layers of bricks is filled with thermal insulation material; in the third solution, both the space between the brick layers and the holes of the inner brick layer are filled with thermal insulating material.

© 2003 Elsevier Ltd. All rights reserved.

*Keywords:* Heat transfer; Moisture diffusion; Condensation; Boundary Element Method

## 1. Introduction

The presence of condensation is one of the main sources of pathologies in buildings [1,2]. Pathologies due to condensation may range from the simple appearance of moulds to the deterioration of the building material itself. To avoid these undesirable phenomena, it is imperative to detect the presence of condensation and to take corrective measures. This detection should occur during the design phase.

Previous researchers have proposed several methods to deal with the problem of heat and moisture transfer. Krischer [3], for instance, identified two transport mechanisms for material moisture in porous materials under the influence of temperature gradients. One of them is named vapour diffusion and the other is usually described as capillary water movement. Luikov [4], and Philip and de Vries [5] also worked with porous materials, and proposed transport moisture models based on the thermodynamics of irreversible processes. An extensive review of these methods may be found in the works of Kießl [6], Kießl and Gertis [7] and Künzl [8].

Glaser [9] proposed a method to identify the condensation risk zones over construction elements subjected to steady-state conditions of heat and vapour diffusion. This method is based on a number of assumptions, namely that only moisture in a vaporized state may be transported, and that this movement occurs in accordance with Fick's law, while heat transfer obeys Fourier's law. Material properties are taken as constant even under condensation conditions. Condensation is assumed to occur when the vapour pressure is equal to the saturated vapour pressure, which is the maximum vapour pressure allowed. In spite of the simplifications assumed by this method, it is frequently used to identify internal condensation risks and to define standards of quality to be met by construction elements. The method of Glaser is even proposed by the DIN 4108 [10] and EN ISO 13788 [11] standards to define condensation. For a good review of the Fourier, and Fick laws see also Carslaw and Jaeger [12], Crank [13] and Gebhart [14].

The Glaser approach is most commonly used in its one-dimensional mathematical formulation. This formulation provides good results when applied to straight elements, with constant thickness and subject to uniform hygrothermal conditions on both sides. However, a one-dimensional formulation is often not accurate enough for solving civil engineering problems. Numerical techniques such as

\* Corresponding author. Tel.: +351-239-797-201; fax: +351-239-797-190.

E-mail address: [tadeu@dec.uc.pt](mailto:tadeu@dec.uc.pt) (A. Tadeu).

the Finite Elements (e.g. [15]), Finite Differences (e.g. [16]) and Boundary Element Methods (BEMs) (e.g. [17–19]) have been used to analyse the phenomena by using two-dimensional model approaches.

The BEM is possibly the best way to analyze heat and moisture diffusion problems, because it allows a compact description of the medium in terms of boundary elements at the material discontinuities alone. However, it leads to a fully populated system, while other techniques, such as the Finite Difference and Finite Element, yield a sparse equation system. In spite of this apparent disadvantage, the reduction of the matrix size of the system produced by the BEM makes the technique efficient.

Thermal resistance is not usually constant along a building envelope. There are zones where this parameter varies considerably, due to the presence of a material (or materials) with differing thermal conductivity. The zones where thermal resistance is lower are commonly known as ‘thermal bridges’, and it is here that condensation first occurs, because heat flux tends to concentrate in these areas. The vapour-pressure gradient found in thermal bridges causes moisture, in its vapour phase, to migrate from one side of the envelope element to the other (e.g. [16]). When the outside environment is colder, the inside surface on thermal bridges has a lower temperature than the surrounding zones, which forces a fall in the maximum amount of vaporized water that can be maintained. The likelihood of condensation occurring thus increases. The best way to counteract the problems caused by thermal bridges is to homogenise thermal resistance throughout the envelope. One way of achieving this is by adding a layer of less conductive material close to the area in question (e.g. [2]).

The consequences of a thermal bridge are usually assumed to concern only those construction elements with high thermal conductivities, such as concrete columns and beams. It is usually assumed that construction elements such as brick walls do not lead to this kind of problems. However, it is possible to find construction brick walls containing coloured stains, which may indicate the existence of associated hygrothermal problems. The present work aims to determine if the type of modelling of a brick wall has an impact on the correct identification of places where condensation may arise.

The present paper uses the BEM to analyse two different models: in the first one, the wall is assumed to be constituted by a set of homogeneous layers, bonded together; while in the second, the geometrical properties of the individual bricks and bonds are modelled. Temperature (and consequently vapour saturation pressure) and vapour pressure distribution maps were developed, allowing the approximate location of condensation risk zones to be predicted. In the examples provided, the heat and moisture diffusion equilibrium are computed first. Then, the vapour saturation pressure distribution is defined, and the zones where the vapour pressure exceeds the vapour saturation pressure, that is where the risk of condensation exists, are identified.

Results yielded by the two models are then compared and discussed.

The article is organised as follows: first, a brief definition of the problem is given, and then the BEM is formulated, indicating the Green’s functions required. The results are then validated using a two-dimensional model wall subjected to one-dimensional steady-state heat and vapour diffusion, for which the analytical solution is known. The BEM formulation is then applied to compare the steady-state heat and moisture diffusion behaviour across double brick walls provided by the two models described above.

## 2. Problem statement

Consider an isotropic medium, assuming steady-state heat and vapour transfer conditions, with no internal heat or moisture generation. Heat conduction and moisture diffusion are governed by the Laplace equation:

$$\frac{\partial^2 V}{\partial x^2} + \frac{\partial^2 V}{\partial y^2} = 0, \quad (1)$$

where  $V$  is the variable field, and  $x$  and  $y$  define the Cartesian coordinate system used.

Fick and Fourier laws are used to study vapour diffusion and heat conduction, respectively, and can be expressed by

$$\vec{v} = -\delta \vec{\nabla} V, \quad (2)$$

where  $\delta$  is the material’s vapour permeability ( $\pi$ ) or the material’s conductivity ( $\lambda$ ) and  $\vec{\nabla} V = (\partial V / \partial x) \vec{e}_1 + (\partial V / \partial y) \vec{e}_2$  is the variable field gradient.

Once vapour pressure and temperature distributions along the medium are known, the maximum vapour pressure that can be maintained at each point must be determined. This parameter is termed vapour saturation pressure, and its value is strongly influenced by the temperature. When the temperature at a given point drops below a certain value, the vapour pressure reaches the saturation pressure value, and condensation occurs. In this work, and according to BS 5250 [20], it is assumed that the relation between temperature and vapour saturation pressure may be expressed by

$$p_s = 610.5e^{(17.269T)/(237.3+T)}, \quad (3)$$

where  $T$  is the temperature.

The condensation risk zones are those where the existing vapour pressure estimated by the Laplace equation equals the vapour saturation pressure.

## 3. Boundary element formulation

The fundamental equations underlying the application of boundary elements to the solution of heat and moisture transfer problems are well known (e.g. [21,22]). The method requires Green’s functions and their derivatives to be integrated for all the elements used to model the problem

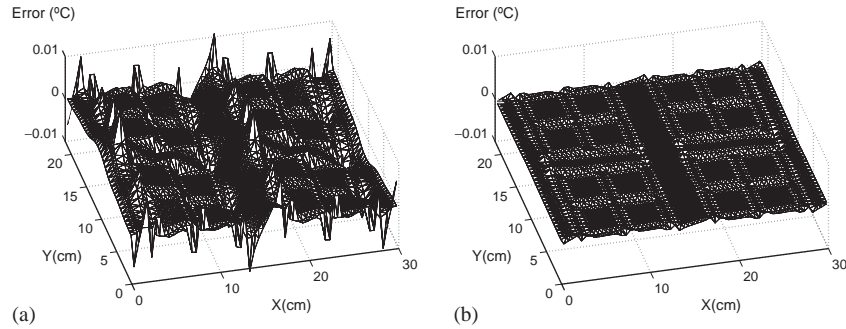


Fig. 1. Validation Model BEM error: (a) 612 elements and (b) 984 elements.

in question:

$$G^{kl} = \int_{C_l} \phi G(x_k, x_l) dC_l, \quad (4)$$

$$H^{kl} = \int_{C_l} \phi H(x_k, x_l, n_l) dC_l \quad (5)$$

in which:  $G(x_k, x_l)$  is the component of the Green's function for temperature or moisture, and  $H(x_k, x_l, n_l)$  is the corresponding flux component at  $x_k$  due to a concentrated load at  $x_l$ ,  $n_l$  is the normal outward unit for the  $l$ th boundary segment  $C_l$ , and  $\phi$  is an interpolation function. For a homogeneous medium, the required Green's function is (e.g. [21,22])

$$G(x, x_0) = 1/(2\pi\delta) \ln(1/r), \quad (6)$$

where  $r$  is the distance between the source and the receiver and  $\delta$  is the material's property (thermal conductivity or vapour permeability), which is taken to be constant.

The corresponding expressions for the flux component are obtained from  $G$  by taking partial derivatives in relation to the unit outward normal direction  $n$ , and then applying Fourier's law

$$H(x, x_0, n_l) = -1/(2\pi) \frac{\partial \ln(1/r)}{\partial n}. \quad (7)$$

### 3.1. Element integration

When the element to be integrated in Eqs. (4) and (5) differs from the loaded element, the integrands are non-singular and the integrations are best carried out using standard Gaussian quadrature. For the loaded element, however, the integrands exhibit a singularity, but it is possible to carry out the integrations in closed form.

Manipulating the integral equations and subjecting them to the continuity conditions at the interface between the two media produces a system of equations that can be solved for the nodal temperatures and heat fluxes. Values for the variable  $V$  or its derivatives at any point in the domain, are obtained, once the nodal temperatures and heat fluxes are known.

### 3.2. BEM validation

The validation of the BEM algorithm is made by applying it to a simple one-dimensional model for which the analytical solution is known. This model is obtained by ascribing constant material properties to the interior of a double brick wall, to simulate the existence of a homogeneous wall. The wall is modelled with the full discretization of the bricks' geometry, as used in the application examples, using discontinuous linear boundary elements.

The inner surface of the wall is kept at a constant temperature  $T_1 = 20.0^\circ\text{C}$ , and the outer surface at temperature  $T_2 = 0.0^\circ\text{C}$ . The heat flux is assumed to be null along the wall, thus defining a one-dimensional steady-state problem and leading to a linear temperature variation across the wall.

The response was calculated over a fine grid, both analytically and using the BEM. Fig. 1a illustrates the error resulting when the model discretization uses 612 boundary elements. Fig. 1b shows the error for a 984 boundary elements model. In each case, the error obtained is very slight, and it decreases as the number of elements is increased, indicating that the BEM performs well.

## 4. Applications

The present work analyses the steady-state heat and moisture diffusion across a double brick wall, composed of two layers of 8-hole ( $4 \times 4 \text{ cm}^2$ ) clay bricks 11 cm-thick, separated by a 4 cm-thick layer. This separation layer may be composed entirely of air or filled with a thermal insulating material.

The exterior and interior faces of the wall are coated with 2 cm of plaster mortar. Fig. 2 shows the geometry of the model and the grid where the results are computed.

As stated above, Model 1 represents a simplification commonly used in heat and moisture transference analysis. The wall is taken as a set of homogeneous layers. In this model, the heat flux across the wall is one dimensional, and perpendicular to the external faces of the wall. On the top and bottom boundaries of the model, null fluxes are prescribed. In Model 2, the real geometry of the brick wall

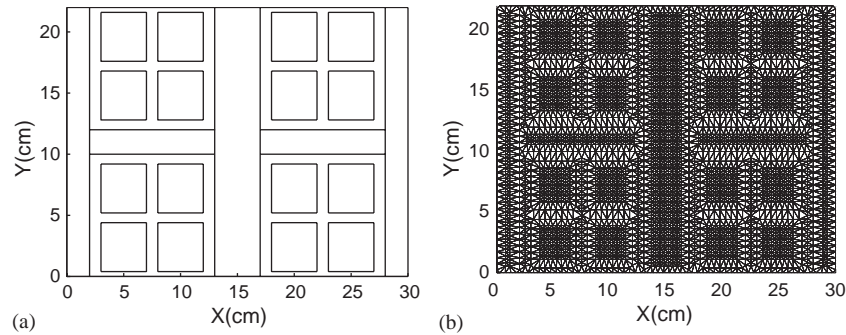


Fig. 2. Application model: (a) Geometry of the model and (b) grid mesh used.

Table 1  
Thermal conductivity and vapour permeability values

Material	$\pi$ (Kg Pa <sup>-1</sup> m <sup>-1</sup> )	$\lambda$ (W °C <sup>-1</sup> m <sup>-1</sup> )
Brick (width –11 cm) <sup>a</sup>	7.24E – 12	0.528
Brick with insulation <sup>a</sup>	2.06E – 12	0.348
Mortar	4.50E – 12	1.150
Insulating material	1.50E – 12	0.035
Air	2.00E – 14	0.235
Brick clay	2.40E – 12	1.150

<sup>a</sup>These values represent global parameters for the full brick taking into account the individual contributions of the clay, mortar and air/insulating material.

was modelled, assuming different hygrothermal property values for the different materials. The BEM discretization is the same for both models. Thus, the discretization chosen allows the full brick geometry to be taken into account in Model 2. The material discontinuities were discretized using 984 linear boundary elements with a length of approximately 5 mm.

The global thermal conductivity and vapour permeability for each bricklayer in Model 1 were defined taking into account the individual contributions of the different materials (e.g. [23,24]).

In both models, the temperature of the right face of the wall is taken to be 20°C, simulating an indoor environment, while the temperature of the left face is kept at 0°C, simulating an outdoor environment. The values for vapour pressure at the inner and outer faces are assumed to be 2103.3 and 518.9 Pa, corresponding to a relative humidity of 90% and 85%, respectively. Table 1 lists the thermal conductivity and vapour permeability values for the materials used in both models.

Two additional fictitious layers, one internal ( $\lambda = 0.1667$  W °C<sup>-1</sup> m<sup>-1</sup>) and the other external ( $\lambda = 0.5$  W °C<sup>-1</sup> m<sup>-1</sup>), each 2 cm thick, are added to the two faces of the wall models to simulate the internal and the external thermal surface resistance, ( $1/h_i = 0.12$  m<sup>2</sup> °C W<sup>-1</sup> and  $1/h_e = 0.04$  m<sup>2</sup> °C W<sup>-1</sup>), respectively. This procedure allows the radiation and convection contributions to be taken into account.

In each model, three different constructive solutions are analysed for different thermal insulation conditions. First, the computations assume the non-existence of thermal insulating material. Then, the space between the two bricklayers is filled with thermal insulating material. Finally, the air holes on the internal bricklayer are filled with thermal insulating material, in addition to the space between the two bricklayers.

Next, for each constructive solution, the temperature and vapour pressure distribution obtained with the first model, and the differences between the two models are displayed as three-dimensional plots. Since the boundary element discretization is kept constant for both models, the disparities arise from the different modelling used for bricks. Additionally, the internal zones where the vapour pressure exceeds the vapour saturation pressure, denominated here as the condensation risk zones, are plotted for both models. These plots use a grey scale, which ascribes bigger differences to darker colours.

#### 4.1. Non-existence of thermal insulating material

Fig. 3 shows the results obtained when no thermal insulating material is present in the double brick wall. As expected, the temperature distribution across the wall exhibits a slightly higher gradient in the air layer, since the thermal conductivity of the air is lower than that of the brick. The maximum difference between temperatures provided by the two models is 0.49°C, and it is located in the vicinity of the brick holes faces (see Fig. 3a). Fig. 3b1 displays the vapour pressure equilibrium results. Again, the bigger differences are located in the close vicinity of the brick holes faces (147.3 Pa).

Figs. 3c1 and c2 display the zone of possible condensation predicted by both models. Model 1, built as a set of juxtaposed layers, indicates a bigger condensation risk area at the external brick layer in the vicinity of the air layer, and at the internal face of the double brick wall (see Fig. 3c1). Meanwhile, Model 2, predicts higher probability of condensation in the left faces of the brick holes, in the side of the outdoor environment. This phenomenon is observable not

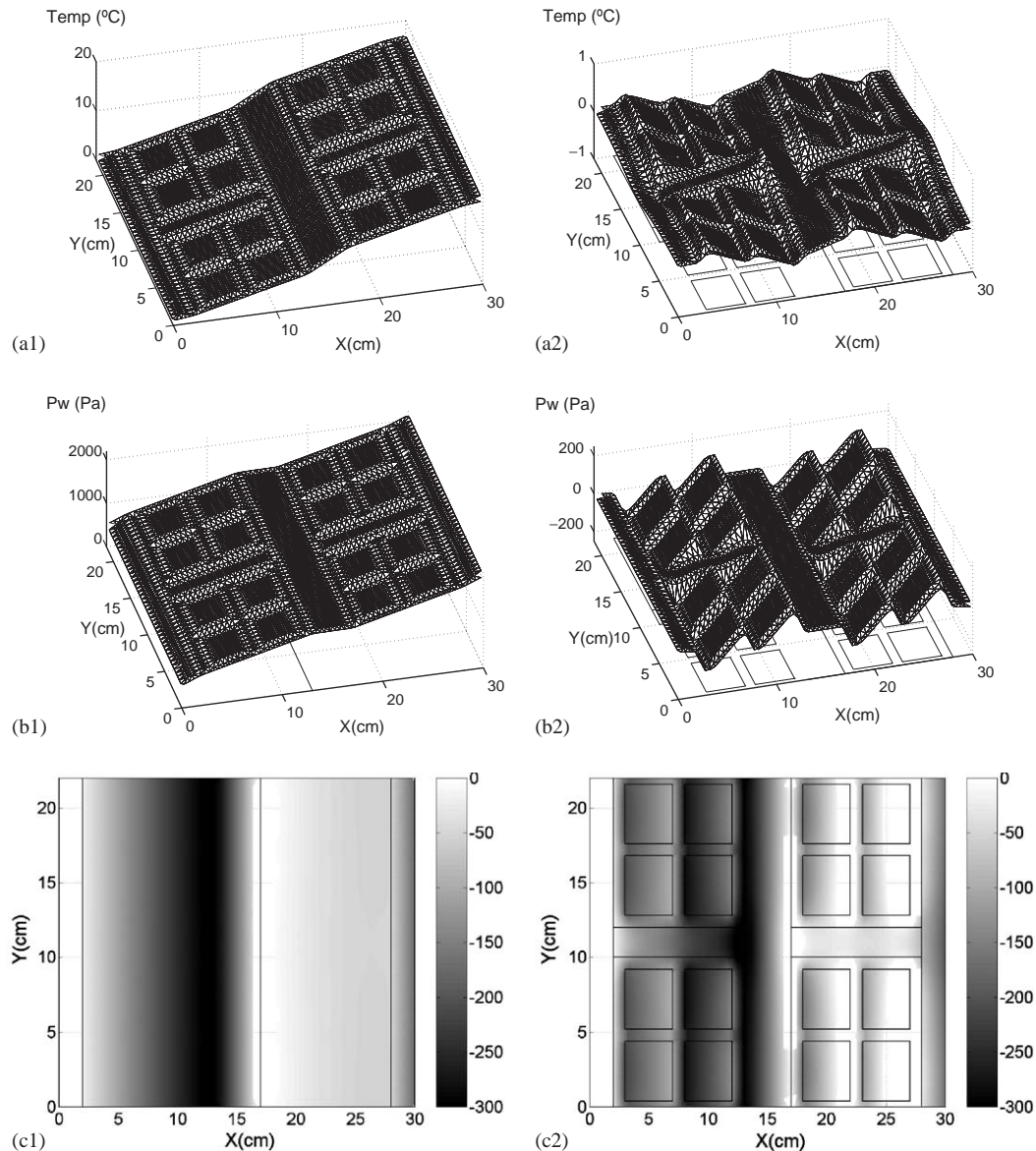


Fig. 3. Double brick wall without thermal insulating layer: (a1) Temperature distribution (Model 1). (a2) Temperature differences between Models 1 and 2. (b1) Vapour pressure distribution (Model 1). (b2) Vapour pressure differences between Models 1 and 2. (c1) Condensation risk zone (Model 1). (c2) Condensation risk zone (Model 2).

only in the air inside the hollow brick holes on the left brick wall, but also on the right brick wall.

The bridge effects along the bricks may be observable in Model 2, along the horizontal mortar strip between the two bricks (see Fig. 3c2), leading there to higher risk of condensation.

#### 4.2. Thermal insulating material between the two bricks layers

Fig. 4 shows the results yielded when a thermal-insulating layer is placed between the two bricklayers. As expected, higher temperature and vapour gradients are observed in the thermal insulating layer, which also happens to be less

permeable to vapour. The temperature distribution along the thermal insulating layer does exhibit a higher temperature gradient than that of the previous example, since the insulating material has a lower thermal conductivity than air. Figs. 4a2 and b2 illustrate the differences obtained between Models 1 and 2. These differences keep the same tendency found in the previous example, but exhibiting now smoother values. The larger temperature and vapour pressure differences are  $0.26^{\circ}\text{C}$  and  $90.4\text{ Pa}$ , respectively. Once again, these divergences occur because the heat and vapour fluxes within the double brick wall (Model 2) are not one-dimensional.

The risk of condensation is now restricted to the left brick-layer and the left side of the insulating layer. As in the

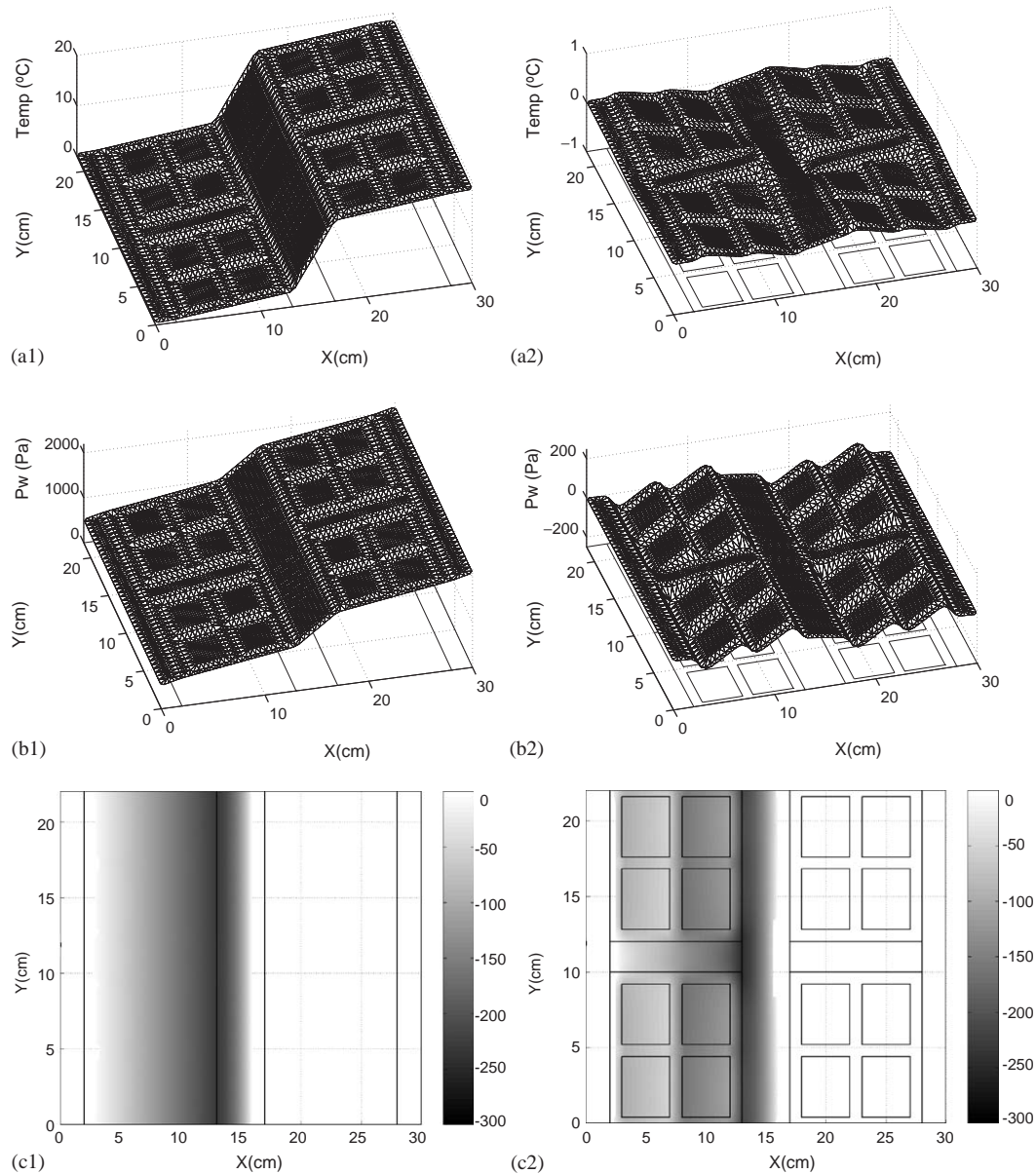


Fig. 4. Double brick wall with a thermal insulating layer between the two brick walls: (a1) Temperature distribution (Model 1). (a2) Temperature differences between Models 1 and 2. (b1) Vapour pressure distribution (Model 1). (b2) Vapour pressure differences between Models 1 and 2. (c1) Condensation risk zone (Model 1). (c2) Condensation risk zone (Model 2).

preceding example, there is a larger tendency for condensation to occur on the inner left face of the brick holes (see Figs. 4c1 and c2). However, the difference between the vapour pressure and the vapour saturation pressure is smaller than in the previous example. Again, the bridge effects along the horizontal mortar strip referred above are clearly visible (see Fig. 4c2).

#### 4.3. Thermal insulating material between the two bricklayers and inside the holes on the right brick layer

Finally, Fig. 5 illustrates the results for a double brick wall with a thermal insulating layer, assuming that the holes on

the right brick layer are also filled with thermal insulating material. The temperature distribution obtained for Model 1 (Fig. 5a1) is similar to that found for the previous examples. The larger temperature differences between the two models are located along the horizontal mortar strip, in its inner zone ( $0.62^{\circ}\text{C}$ ).

The vapour pressure gradients along the inner (right) bricklayer and across the insulating layer are similar, without the differences registered in the previous examples (see Figs. 5b1, 4b1 and 3b1). The vapour pressure differences between Models 1 and 2 are now smoother, with a maximum of 64.5 Pa along the inner part of the left brick layer (see Fig. 5b2).

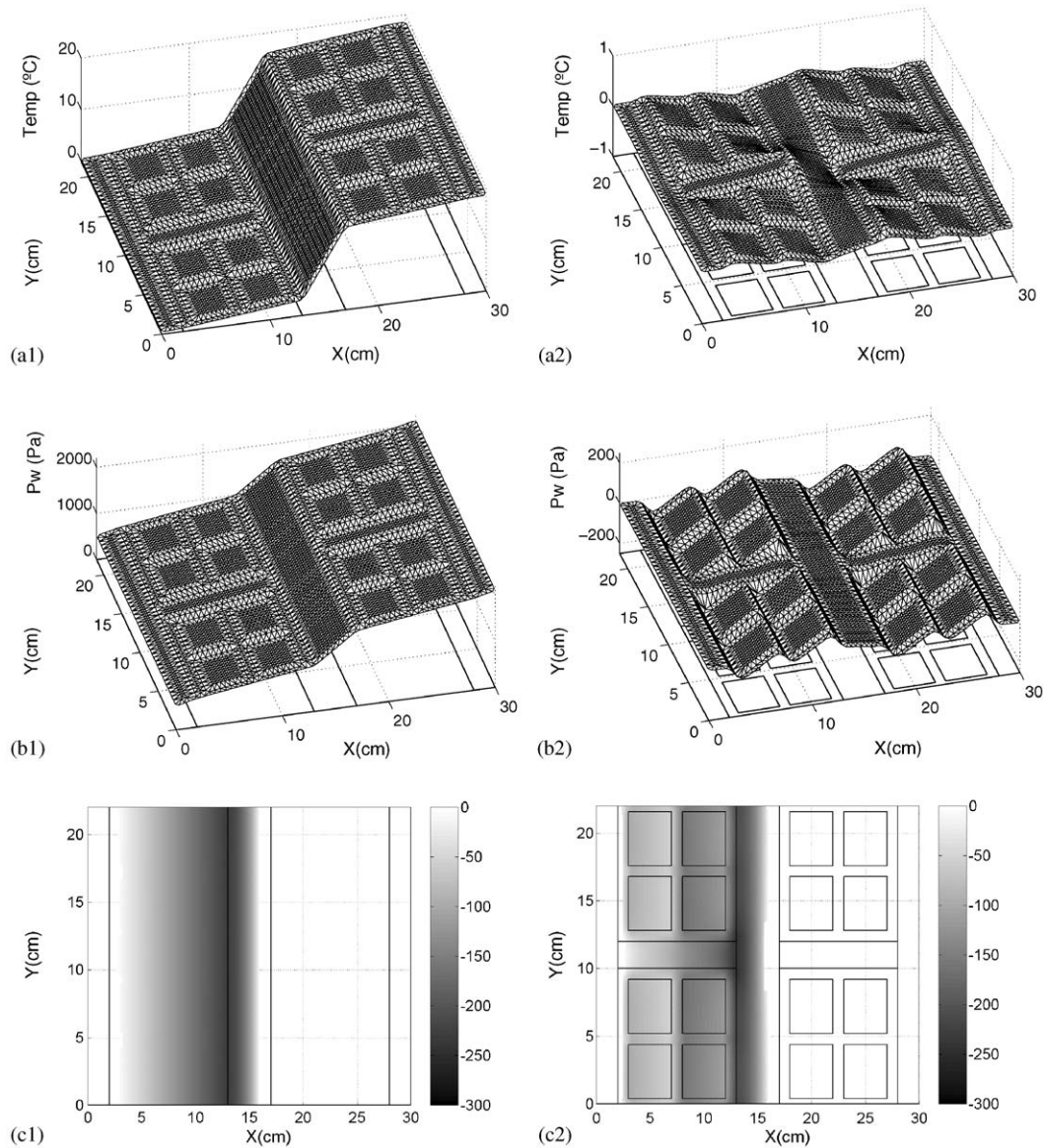


Fig. 5. Double brick wall with thermal insulating material between the two bricklayers and inside right layer brick holes. (a1) Temperature distribution (Model 1). (a2) Temperature differences between Models 1 and 2. (b1) Vapour pressure distribution (Model 1). (b2) Vapour pressure differences between Models 1 and 2. (c1) Condensation risk zone (Model 1). (c2) Condensation risk zone (Model 2).

The condensation risk zones are smaller than in the previous examples, as expected given the presence of additional thermal insulating material. Both models predict risk of condensation in the inner part of the left bricklayer. Again, the thermal bridge behaviour generated by the horizontal mortar strip between the bricks is easily observable when the different material properties of the brick are taken into account (Model 2—see Fig. 5c2).

## 5. Conclusions

The Boundary Element Method (BEM) has been formulated and implemented to solve two-dimensional heat

conduction and vapour diffusion problems efficiently. After the validation of the method, the BEM was used to study the heat and moisture diffusion across a double brick wall.

Several constructive solutions were analysed, with two different BEM discretization models. The first model assumes the existence of a set of homogeneous layers, bonded together, while in the second, the geometrical and hygrothermal properties of the individual bricks and bonds are modelled. Temperature (and consequently vapour saturation pressure) and vapour pressure maps across the double brick wall were then produced, in order to predict the zones where the risk of internal condensation exists.

The results suggest that both methods differ when defining the vapour pressure within double brick walls. Larger

differences are found when the amount of thermal insulating diminishes. Our results reveal that the horizontal mortar strip between bricks behaves as a thermal bridge. This result is only observable when the modelling of the brick takes into account the several brick material properties.

The divergences between both models lead to different condensation risk areas being predicted by them. The simplified one-dimensional model (Model 1), proves to be more pessimistic than the two-dimensional one when calculating the risk of condensation in the inner part of the exterior brick layer, close to the cavity separating the two brick layers. On the other hand, Model 2 is more pessimistic in the prediction of the condensation risk in the vicinity of the brick holes placed close to the exterior face of the double brick wall.

## References

- [1] Freitas V. Condensations in Portuguese buildings. Proceedings of the International Symposium on Moisture Problems in Building Walls, Porto, Portugal, 1995. p. 75–85.
- [2] Aroso MH. Moisture condensation in thermal bridges. Establishing design criteria. Proceedings of the International Symposium on Moisture Problems in Building Walls, Porto, Portugal, 1995. p. 86–96.
- [3] Krischer O, Kast W. Die wissenschaftlichen Grundlagen der Trocknungstechnik. Dritte Auflage. Berlin: Springer; 1978.
- [4] Luikov AV. Systems of differential equations of heat and mass transfer. International Journal of Heat and Mass Transfer 1975;18: 1–14.
- [5] Philip JR, de Vries DA. Moisture movement in porous materials under temperature gradients. Transactions, American Geophysical Union 1957;2:222–32.
- [6] Kießl K. Kapillarer und dampfförmiger Feuchtetransport in mehrschichtigen Bauteilen. Dissertation, Universität-Gesamthochschule Essen, 1983.
- [7] Kießl K, Gertis K. Feuchtetransport in Baustoffen. Forschungsberichte aus dem Fachbereich Bauwesen. Dissertation Universität-Gesamthochschule Essen, 1980.
- [8] Künzel HM. Simultaneous heat and moisture transport in building components. One- and two-dimensional calculation using simple parameters. Stuttgart: IRB Verlag; 1995.
- [9] Glaser H. Vereinfachte Berechnung der Dampfdiffusion durch geschichtete Wände bei Ausscheidung von Wasser und Eis. Kältetechnik 1958;10(11):358–64 and 10(12):386–90.
- [10] DIN 4108-Wärmeschutz im Hochbau. DIN Deutsches Institut für Normung, 1981.
- [11] GTR WI 46 and CEN/TC 89 WI29. EN ISO 13788-Hygrothermal performance of building components and building elements. Internal surface temperature to avoid critical surface humidity and interstitial Condensation. Calculation methods, 2000.
- [12] Carslaw HS, Jaeger JC. Conduction of heat in solids, 2nd ed. Oxford: Oxford Science Publications, Clarendon Press; 1997.
- [13] Crank J. The mathematics of diffusion, 2nd ed. Oxford: Oxford Science Publications, Clarendon Press; 1999.
- [14] Gebhart B. Heat conduction and mass diffusion. Singapore: International Editions, McGraw-Hill Inc Publications; 1993.
- [15] Bathe KJ. Numerical methods in finite element analysis. Englewood Cliffs, NJ: Prentice-Hall; 1976.
- [16] Freitas V, Abrantes V, Crausse P. Moisture migration in building walls. Analysis of the Interface Phenomena. Building and Environment 1996;31(2):99–108.
- [17] Fratantonio M, Rencis JJ. Exact boundary element integrations for two-dimensional Laplace equation. Engineering Analysis with Boundary Elements 2000;24(4):325–42.
- [18] Ochiai Y, Sekiya T. Steady state heat conduction analysis by improved multiple-reciprocity boundary element method. Engineering Analysis with Boundary Elements 1996;18(2):111–7.
- [19] Melnikov YA. An alternative construction of Green's function for the two-dimensional heat conduction. Engineering Analysis with Boundary Elements 2000;24(6):467–75.
- [20] BS 5250-British Standard 5250. Appendix B, 1989.
- [21] Brebbia CA, Dominguez J. Boundary elements. An introductory course. Boston: Computational Mechanics Publications and New York: McGraw Hill Book Company, 1989.
- [22] Manolis GD, Beskos DE. Boundary element methods in elastodynamics. London: Unwin Hyman (sold to Chapman and Hall); 1988.
- [23] Santos CA, Paiva JA. Coeficientes de Transmissão Térmica de Elementos da Envolvente dos Edifícios (Thermal transmission coefficients of building elements). Informação Técnica de Edifícios 28. Lisbon, Portugal: Laboratório Nacional de Engenharia Civil; 1996.
- [24] Freitas V. Permeabilidade ao Vapor de Materiais de Construção. Condensações Internas (Vapour permeability of construction materials. Internal condensation). Nota de Informação Técnica—NIT 002. Oporto, Portugal: Civil Engineering Department, University of Oporto; 1998.